Dynamics of formation of *K*-hole fractions of sulfur projectiles inside a carbon foil

J. Braziewicz,[1,*] U. Majewska,[1] K. Słabkowska,[2] M. Polasik,[2] I. Fijał,[3] M. Jaskóła,[3] A. Korman,[3] W. Czarnacki,[3] S. Chojnacki,[4] and W. Kretschmer[5]

[1]*Institute of Physics, Świętokrzyska Academy in Kielce, 25-406 Kielce, Poland*
[2]*Faculty of Chemistry, Nicholas Copernicus University, 87-100 Toruń, Poland*
[3]*The Andrzej Soltan Institute for Nuclear Studies, 05-400 Otwock-Świerk, Poland*
[4]*Heavy Ion Laboratory, Warsaw University, 02-097 Warsaw, Poland*
[5]*Physikalisches Institut, Universität Erlangen-Nürnberg, D-91058 Erlangen, Germany*

(Received 4 December 2003; published 7 June 2004)

The $K\alpha$ and $K\beta$ satellite and hypersatellite x-ray lines emitted by highly ionized sulfur projectiles passing with energies from 65 MeV up to 122 MeV through carbon foils of thickness of 15-210 μg cm^{-2} have been recorded using a Si(Li) detector. The additional hypersatellite Ky^h peak proves that for such high energies of the sulfur ions very high subshells ($4p$ and $5p$) could be occupied. In order to study the dynamics of formation of *K*-shell vacancy fractions of sulfur projectiles passing through a carbon foil the dependence of sulfur *K* x-ray production cross sections on foil thickness has been examined separately for each recorded line using the three component model. For each projectile energy the values of *K*-shell hole production cross sections and *K*-shell electron capture cross sections (both common for all recorded x-ray lines in the case of each projectile energy) have been fitted, as well as the specific values (for each recorded x-ray line) of *K*-shell hole filling cross sections, which are directly connected with average lifetimes of appropriate states of sulfur ions. The obtained "experimental" values of *K*-shell vacancy production cross sections are much higher than the theoretical predictions. This suggests that apart from the ionization process the excitation from *K* shell into higher shells is responsible for a production of *K*-shell vacancies, which has been confirmed by recent classical trajectory Monte Carlo calculations.

DOI: 10.1103/PhysRevA.69.062705 PACS number(s): 34.50.Fa

I. INTRODUCTION

In collisions of heavy ions with target atoms the strong Coulomb field of one of the "collision partners" can cause simultaneous ejection of several electrons of the second one. This process results in a reduction of the nuclear charge screening and increases the binding energy of remaining electrons [1]. Consequently, the energies of x rays emitted from such multiply ionized atoms are shifted with respect to the corresponding x-ray energies of singly ionized atoms and reflect the actual configuration of electrons during x-ray emission. Finally, as a result of the multiple ionization, instead of a single-hole x-ray transition called the diagram line, the structure of x-ray satellites appears.

Collision processes have been studied extensively for many years but these studies were focused mainly on single or multiple *K*-, *L*-, *M*-shell ionization occurring in the target atoms. The satellite structure of *K* and *L* x-ray lines of the target atoms, observed mainly with high resolution spectrometers [2–5], was interpreted as the result of additional vacancies in outer shells of the atom. However, more complicated processes are experienced by a projectile as a second partner of the ion-atom collision. During the first collision *K*-vacancy and/or multiple *L*-, *M*-, *N*- or higher shell vacancies can be produced. Further, the ion can collide with the other target atoms and capture or loss of electrons can occur before its original vacancies are filled by outer electrons. The competition between ionization, excitation, electron capture, electron loss and decay processes leads to the establishment of an electron-vacancy equilibration in different shells of the moving projectile. Collision processes occurring between the swift heavy ions and target atoms have been investigated during past decades [6–13] but most systematic experiments were performed using high resolution measurements of *K* or *L* x rays from different projectiles in solid targets [14–23]. A review of problems discussed and experimental works has been published by Beyer *et al.* [24].

For low resolution x-ray spectrometers, such as a semiconductor Si(Li) detector, the satellite structure of induced x rays cannot be resolved. Nevertheless, the measured x-ray spectra are strongly affected by multiple ionization, namely the x-ray lines are shifted towards higher energies and broadened [25,26] and thus information on probabilities of multiple ionization still can be extracted. The method of analysis of multiple ionization from low resolution x-ray spectra was used in our previous works to study the ionization probabilities for *M*, *N*, and *O* shells of heavy atoms generated by projectiles [25,27–29] and for *K*, *L*, and *M* shells of sulfur projectiles passing through a carbon foil [30]. We have used the fact that the x-ray satellite structure can be well approximated by the Gaussian profile, whose energy shift and width depend on the ionization probability for the *L* and *M* shells at the moment of x-ray emission. In the present paper this method is also used.

The dependence of x-ray production cross sections of heavy ions on foil thickness has been demonstrated in several papers [6,9,23,31–35]. Generally, measured projectile x-ray yields are strongly dependent upon whether or not a *K*

*Electronic address: janusz.braziewicz@pu.kielce.pl

vacancy exists in the incoming ion. In some works it was found that *K* vacancy equilibrium is not reached until the ion passes through many atomic layers in the foil. Indeed, the works of Scharfer *et al.* [36] and Gray *et al.* [37] concerning sulfur ions show directly that the magnitude of *K* vacancy fractions of the ions are dependent on foil thickness. On the other hand, the charge equilibrium state for shells higher than *K* shell is reached very rapidly (in the first few atomic layers), as it was shown by Cocke *et al.* [38]. To describe these results quantitatively a model based on formulation of Allison [39] has been widely applied. Betz *et al.* [6] used a so called "two component" version, in which the beam is considered to consist of two fractions of ions, those with and those without the *K* vacancy. In the case of a collision, when the fraction of ions with two *K* vacancies plays a significant role, Gardner *et al.* [11] have shown that it is necessary to consider a "three-component" version, where the projectile may have zero, one or two *K* vacancies.

The main goal of the present work is to study the dynamics of formation of *K*-shell vacancy fractions of sulfur projectiles passing through a carbon foil. Therefore, we have performed an interpretation of target thickness dependence of measured x-ray production cross sections, for the first time separately for each recorded line ($K\alpha^s_{1,2}$, $K\alpha^h_{1,2}$, $K\beta^s_{1,3}$, $K\beta^h_{1,3}$, Ky^s, and Ky^h) using the three component model. Using this model we have evaluated the values of *K*-shell vacancy production and filling cross sections.

II. EXPERIMENTAL DETAILS

Sulfur ion beams with incident energies of 65, 79, 99, and 122 MeV and with incident charges of 13^+ and 14^+ were obtained from the U-200P cyclotron at the Heavy Ion Laboratory of Warsaw University. The experimental setup applied in this work was the same as that described earlier [30], therefore only a brief description is presented here. Two collimators located at 24 and 38 cm in front of the target are used to define 2 mm in diameter beam spot on the target. Self-supporting carbon foils with effective thickness of 15–210 μg cm^{-2}, were positioned in the target holder at the center of vacuum chamber at an angle of 25° to the direction of the beam. The geometry of the experimental arrangement used in this work means that the detector should register x rays emitted by projectile inside the target as well as from distance up to 1.2 cm behind the target, so during such experiments x rays with lifetimes up to 10^{-12} sec are registered.

The carbon targets were prepared by vacuum evaporation and their absolute thickness was determined in the separate measurements of energy loss of 5.48 MeV α particles from Am source. The stopping power values for α particles in carbon needed to calculate the foil thickness were obtained from Biersack and Maggamark [40] and the final target thickness was calculated by the computer code TRIM [41]. Additionally these thicknesses were checked using elastic scattered 2.0 MeV $^4He^+$ ions from the Van de Graaff accelerator. Absolute target thicknesses were determined with the accuracy of about ±4%. The targets could be considered as "thin" because the ions passing through the foil did not lose energy appreciably (ΔE was less than $0.15E_0$ for the thickest target and for the lowest ion energy and decreased rapidly up to $0.01E_0$ for the highest projectile energy). The effective ion energy was further used. The self-absorption of the measured x rays in a target is also small (less than 4%). Independent measurements of target thickness enabled absolute normalization of the x rays intensity on the incident number of projectiles obtained from elastically scattered sulfur ions detected in a silicon surface-barrier detector located inside the chamber at 12.5° to the beam direction.

The *K* x rays emitted from the moving projectiles were measured in the beam incident side of the target at 90° to the beam direction by a Si(Li) detector (30 mm^2 active area, crystal thickness 5 mm and energy resolution of FWHM = 170 eV for 6.4 keV) placed outside the target chamber. Projectile x rays passed in their way to the detector through 10 μm metallized Mylar chamber window, 25 μm thick beryllium detector window and 5 mm air gap between both windows. Since the registered *K* x rays of the sulfur projectile were attenuated due to transmission through these various absorbers the used x-ray spectrometer was carefully calibrated to obtain its detection efficiency. The calibration was performed in x-ray energy range of 1.5–120 keV using standard calibrating sources of ^{57}Co, ^{133}Ba, ^{152}Eu, ^{241}Am and by *PIXE* measurements of x rays from thin calibrating targets (Z_t=13–42) according to the recipe of Pajek *et al.* [42]. For the relatively low energy region in this work (2–5 keV) the detector efficiency was determined within uncertainty less than 4%. The energetic calibration of the spectrometer (a second sensitive parameter at the present study) was checked several times during experimental runs by measurements of the x rays emitted from standard radioactive sources (^{57}Co, ^{133}Eu, ^{152}Ba, and ^{241}Am) and was determined with an uncertainty of 2–3 eV depending on the experimental run.

III. SPECTRA ANALYSIS PROCEDURE

Typical x-ray spectra recorded by Si(Li) detector for sulfur ions passing with energies of 65, 79, 99, and 122 MeV through a carbon target are presented in Fig. 1. The origin of all recorded peaks is described in detail in our previous paper [30]. The resolved $K\alpha^s_{1,2}$, $K\beta^s_{1,3}$ satellite and $K\alpha^h_{1,2}$, $K\beta^h_{1,3}$ hypersatellite peaks are the results of the overlapped contributions corresponding to transitions of the following types: $1s^{-1}\rightarrow 2p^{-1}$, $1s^{-1}\rightarrow 3p^{-1}$, $1s^{-2}\rightarrow 1s^{-1}2p^{-1}$, and $1s^{-2}\rightarrow 1s^{-1}3p^{-1}$, respectively, from highly ionized sulfur projectiles. For sulfur ions with incident energies of 79–122 MeV an additional highest-energy peak in the measured x-ray spectra labelled as Ky^h (see Fig. 1) has been detected. This peak corresponds to the hypersatellite transitions from the 4*p* and 5*p* subshells (i.e., the transitions of the following types: $1s^{-2}\rightarrow 1s^{-1}4p^{-1}$ and $1s^{-2}\rightarrow 1s^{-1}5p^{-1}$) and proves that the Ky^s satellite transitions (i.e., the transitions of the following types: $1s^{-1}\rightarrow 4p^{-1}$ and $1s^{-1}\rightarrow 5p^{-1}$) also take place. The lack of a separate Ky^s satellite peak in the observed spectra indicates [30] that the contribution of this type of transition must overlap with another peak. The Ky^s peak intensity has been calculated from $K\beta^h_{1,3}$ one according to the procedure described by Majewska *et al.* [30].

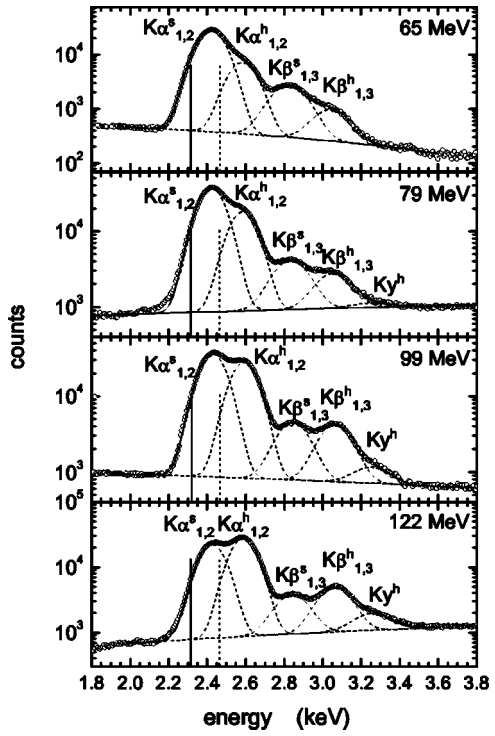

FIG. 1. The *K* x-ray spectra emitted by sulfur projectiles passing with energies of 65, 79, 99, and 122 MeV through a carbon foil with thickness ~150 μg cm^{-2}. Solid and dotted vertical lines show positions of $K\alpha_{1,2}$ and $K\beta_{1,3}$ diagram lines, respectively, while dashed lines show resolved individual transitions according to the method described in the text.

In contrast to the $K\alpha_{1,2}$ and $K\beta_{1,3}$ diagram lines in the x-ray spectrum of the singly ionized sulfur atom, the resolved (see Fig. 1) $K\alpha^s_{1,2}$, $K\beta^s_{1,3}$ satellite and $K\alpha^h_{1,2}$, $K\beta^h_{1,3}$, Ky^h hypersatellite peaks in the x-ray spectrum emitted by multiply ionized sulfur projectiles are broadened and shifted towards higher energies (the widths and energy shifts are characteristic for individual peaks). In this work all x-ray peaks recorded by Si(Li) detector were formed, in fact, by a convolution of a wide (~150 eV) Gaussian response function of the semiconductor detector with the natural structure of the satellite or hypersatellite lines in the *K* x-ray spectrum, having typical energy spacing in the range of tens of eV. In our previous work by Banaś *et al.* [27] we have shown that assuming the binomial character of the intensity distribution of x-ray satellites and taking into account their natural widths and their Gaussian energy spread in the semiconductor detector, the measured x-ray peaks appear as the Gaussian profile which is shifted and broadened with respect to the diagram line. Moreover, we have demonstrated [27] that the energy shift and width of each measured x-ray peak can be expressed in terms of the multiple ionization probabilities and the energy shift per electron vacancy. In the present study we have adopted this method for analysis of the measured *K* x-ray spectra of multiply ionized sulfur projectiles passing through a carbon foil. The energies and intensities of resolved x-ray peaks were determined from a least-square analysis of the spectra using four or five (see Fig. 1) fitting Gaussian functions (with the characteristic width of Gaussian function for each peak) and a polynomial form of the background. The energy shift and width of each x-ray peak reflect the electronic configurations of highly ionized sulfur projectiles at the time of x-ray emission and the results of such studies have been published in our previous papers [30,43].

The measured energies of all of the x rays emitted from the moving ions were corrected for the Doppler effect resulting in transformation of registered energies into the projectile rest frame. The stopping power of sulfur ions in the target was taken into account by using effective beam energy. The measured intensities of the x-ray peaks were corrected for the detector efficiency and for self-absorption of x rays in the target.

IV. RESULTS AND DISCUSSION

The satellite and hypersatellite x-ray production cross sections (marked as $\sigma_{K\alpha^s_{1,2}}$, $\sigma_{K\beta^s_{1,3}}$, σ_{Ky^s}, $\sigma_{K\alpha^h_{1,2}}$, $\sigma_{K\beta^h_{1,3}}$, and σ_{Ky^h}) have been calculated as a result of the normalization of the measured x-ray lines intensities on the number of projectiles and effective target thickness. The cross sections dependence on target thickness for all projectile energies is presented in Fig. 2. Such behavior reflects the dynamics of creation and disappearance of *K*-vacancy fractions of sulfur ions passing through a carbon target. The x-ray production cross section, being a result of x-ray emission by projectile inside and outside the target, was expressed by a function of the ion equilibrium fraction, the formation and loss *K*-shell vacancy cross sections σ_{ij} [39], the radiation probability per unit path length, the satellite/hypersatellite fluorescence yield of the multiply ionized atom, and the fraction of ions able to emit the x rays in question. This procedure assumes that the x-ray production cross section does not depend on the ion incident charge states, i.e., that electrons in shells higher than *K* achieve the equilibrium very rapidly after entering the foil (in the first few atomic layers). The work of Cocke *et al.* [38] and our recent data [43] show that it is a reasonable assumption.

The equilibrium charge state plays an essential role in the theoretical approach based on the rate equations [see Eq. (1)] [39]. The measurements of *K* x-ray spectra of the fast sulfur projectiles passing through carbon foils of thickness in the range of 15-210 μg cm^{-2} allow us to study the equilibrium charge state in all shells. The thickest foils have been chosen to be sure that for such high ion energies the equilibrium charge state will be achieved for most of the sulfur ions inside these foils. The thinner foils have been studied in order to check the influence of the nonequilibrium charge fractions of sulfur ions on the measured *K* x-ray spectra. Mizogawa *et al.* [23] and Shima *et al.* [19] show that the length of the path after which a projectile achieves the equilibrium charge state depends strongly on the beam energy and on the initial charge state of the projectiles. For high ion energy the length of this path increases proportionally to the difference between the initial and the mean equilibrium charge states.

The problem of equilibration of the electron population in various shells of sulfur ions has been explained in our recent work [43] by the analysis of the dependence of the experimental energy shifts and relative intensities of the individual

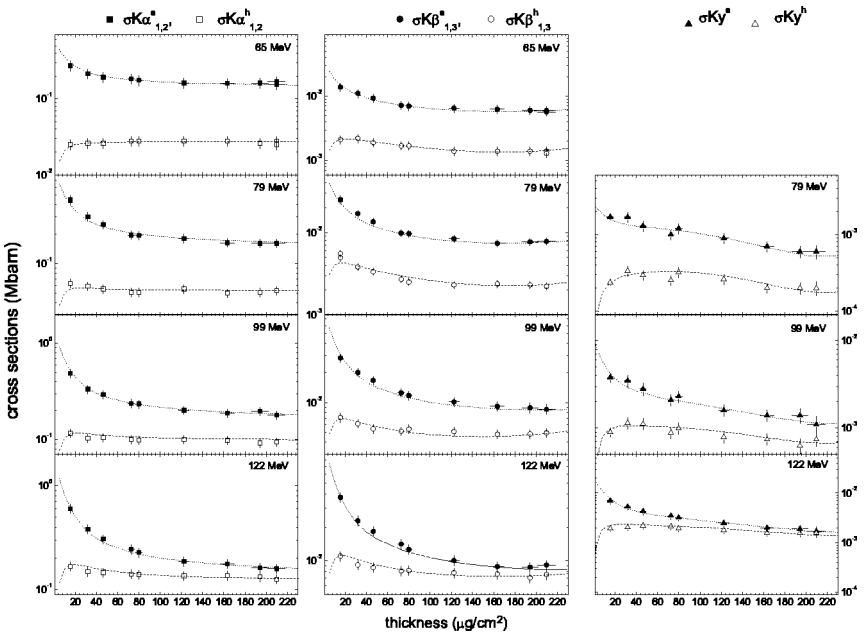

FIG. 2. Dependence of $\sigma K\alpha^{s}_{1,2}$ (solid squares), $\sigma K\alpha^{h}_{1,2}$ (open squares), $\sigma K\beta^{s}_{1,3}$ (solid circles), $\sigma K\beta^{h}_{1,3}$ (open circles), σKy^{s} (solid triangles), and σKy^{h} (open triangles) x-ray production cross sections on the target thickness for the sulfur projectiles with energy 65, 79, 99, and 122 MeV. The smooth curves are the result of least-squares fits, according to the procedure described in the text. Target thickness uncertainties are marked only for satellite data.

K x-ray peaks on the carbon target thickness. It was shown that the measured shifts of the transition energies for the satellite and hypersatellite $K\alpha^{s,h}_{1,2}$, $K\beta^{s,h}_{1,3}$ and $Ky^{s,h}$ x-ray peaks with respect to diagram energies for a singly ionized atom (Bearden [44]) are almost (within error bars $\sim$1.5 eV for $K\alpha^{s,h}_{1,2}$, $\sim$3 eV for $K\beta^{s,h}_{1,3}$ and $\sim$4 eV for $Ky^{s,h}$) independent on the target thickness. Generally, it suggests an insignificant role of the nonequilibrium charge fractions of sulfur ions at L and M shells even in the case of the thinnest carbon foils. The $K\alpha^{h}_{1,2}$:$K\alpha^{s}_{1,2}$ and $K\beta^{h}_{1,3}$:$K\beta^{s}_{1,3}$ intensity ratios allow us to conclude that a rather long path of the projectile inside the carbon target (characteristically increasing with the projectile energy) [43] is required to achieve an equilibrated number of the projectile K-shell electrons. We have shown [43] that for the highest sulfur energies equilibration of the electron population in the K shell of the projectile is achieved for the bulk of sulfur ions in the carbon foil, with thickness not less than 100 μg cm^{-2} [30,43].

To study the dynamics of formation of K-vacancy fractions of the sulfur ions, the description of the projectile x-ray yields is based on the formulation of Allison [39], which expresses the probability of an ion charge-changing collisions by cross sections σ_{ij} (where i represents the initial number of K-shell vacancies and j is their number after event). In the measured energy region multicollisional effects lead to the creation of three fractions of projectiles, i.e., a fraction without a K-shell vacancy (F_0), a fraction with a single K-shell vacancy (F_1) and a fraction with two K-shell vacancies (F_2). In this case a three-component model is used, in which zero, one and two K-vacancy fractions are created and disappear during ion passage through the target. The main assumption of this model is that the beam fractions F_j with K-shell vacancies at any point of the target are related so that $\Sigma_j F_j = 1$ (where $j = 0, 1, 2$). The continuous changing of the charge composition of an ion beam inside a target is expressed by the known rate equations [39], i.e.,

$$\frac{dF_1}{dx} = F_0\sigma_{01} - F_1(\sigma_{10} + \sigma_{12}) + F_2\sigma_{21},$$

$$\frac{dF_2}{dx} = F_0\sigma_{02} + F_1\sigma_{12} - F_2(\sigma_{20} + \sigma_{21}),$$

$$F_0 + F_1 + F_2 = 1. \tag{1}$$

Their solution gives yields of anticipated K-shell vacancy fractions at target thickness x of the form

$$F_j(x) = F_{j\infty} + P(i,j)e^{f_1(\sigma_{ij})x} + N(i,j)e^{-f_2(\sigma_{ij})x}, \tag{2}$$

where $F_{j\infty}$ is the equilibrium fraction of ions with j K-shell vacancies, $P(i,j)$, $N(i,j)$ are functions of the boundary conditions with i equal to the initial number of K-shell vacancies in the entering projectile and j equal to the number of K-shell vacancies under consideration, and f_1 and f_2 are functions of K-shell charge changing cross sections σ_{ij} (i.e., the formation and loss of K-shell vacancy cross sections).

The total intensity of x rays emitted by the projectiles may be written in terms of the contribution from the individual projectile K-vacancy fractions and these contributions should consider the place of x-rays emission, i.e., "inside" and "outside" the foil. To describe the x-ray satellite and hypersatellite intensities registered in the present work we formulate an expression of the measured appropriate intensity $dN_l^{(s,h)-ins}$ arising inside the foil at distance x in an elemental thickness dx as

$$dN_l^{(s,h)-ins}(x) = I_0F_j(x)\lambda_l^{s,h}R_l^{s,h}dx, \tag{3}$$

where $l = K\alpha^{s,h}_{1,2}$, $K\beta^{s,h}_{1,3}$ or $Ky^{s,h}$ x-ray transitions, I_0 is the total number of bombarding ions, $\lambda_l^{s,h}$ is the radiation probability per unit path length (in unit of cm^2) for satellite or hypersatellite transitions, $F_j(x)$ is the fraction of ions at distance x with one ($j=1$ for satellite) or two ($j=2$ for hypersatellite) K-shell vacancies described by Eq. (2) and $R_l^{s,h}$ is a fraction of ions able to emit l x rays, i.e., having one electron in the $2p$, $3p$ or $4p$ subshells.

According to the expression

$$N_l^{(s,h)-out} = I_0 F_j(x_o)\omega_l^{s,h} R_l^{s,h}, \tag{4}$$

the emission of x rays outside the foil is determined by projectile fraction $F_j(x_o)$, which emerges from the foil of thickness x_o. The $\omega_l^{s,h}$ is the satellite/hypersatellite fluorescence yield of the multiply ionized atom. If an ion has two *K*-shell vacancies at the exit of the foil it can emit a hypersatellite x ray and then a satellite x ray if the ion has more than one outer shell electrons. However, this x-ray emission cascade is not included, as in measured ion energies the needed electron configurations are negligible [30].

The result of integration of Eq. (3) over foil thickness x_o in conjunction with Eq. (4) gives an expression for the *K* x-ray production cross section of particular satellite $K\alpha_{1,2}^s$, $K\beta_{1,3}^s$, Ky^s or hypersatellite $K\alpha_{1,2}^h$, $K\beta_{1,3}^h$ and Ky^h transition as

$$\begin{aligned}\sigma_l^{s,h}(x_o) = \lambda_l^{s,h} R_l^{s,h}\{F_{j\infty} - (P/f_1 x_o)(1 - e^{f_1 x_o}) + (N/f_2 x_o)(1 \\ - e^{-f_2 x_o})\} + \omega_l^{s,h} R_l^{s,h}/x_o\{F_{j\infty} + Pe^{f_1 x_o} + Ne^{-f_2 x_o}\} \\ = \{N_l^{(s,h)-ins}(x_o) + N_l^{(s,h)-out}(x_o)\}/(x_o I_o).\end{aligned} \tag{5}$$

In this equation it is assumed that $\sigma_l^{s,h}$ cross section does not depend on the ion incident charge states, i.e., electrons in shells higher than the *K* shell equilibrate very rapidly in the first few atomic layers. This assumption holds very well in the full range of target thicknesses used. Contrary to some works discussing this problem [12,37] in the present study we try to reproduce the dependence of experimental values of $K\alpha_{1,2}^{s,h}$, $K\beta_{1,3}^{s,h}$ and $Ky^{s,h}$ production cross sections on foil thickness, for the first time using three component model separately.

The charge-changing cross sections were fitted to the measured x-ray production cross sections using the values of fluorescence yields $\omega_l^{s,h}$. Because in our experiment different x-ray lines are emitted practically from different ions with a few electrons in different electron defect configurations (with frequency defined by $R_l^{s,h}$) the fluorescent yield is defined (see below) separately for more frequent electronic configurations and is called "effective fluorescent yield." It should be pointed out that fluorescence yield depends strongly on the ionization state of the outer shells. This effect is very important in the framework of the present paper where multiple ionization of sulfur outer shells is essential and varies substantially in the whole range of projectile energy. The fluorescence yield of the singly ionized atom [45,46] is not adequate in our case. Therefore, the theoretical estimation of the "effective fluorescence yield" for a particular type of electron transition (l) for multiply ionized projectile was obtained using the scaling procedure of Larkins [47], namely

$$\omega_l^s = \frac{\sum_{r(l)} \Gamma_{x_{r(l)}} \frac{n_r}{N_r}}{\sum_i \Gamma_{x_i} \frac{n_i}{N_i} + \sum_{i \leqslant j} \Gamma_{A_{ij}} \frac{n_i}{N_i} \frac{m_j}{M_j}}. \tag{6}$$

In this equation the summation in the numerator runs over possible transitions $r(l)$ creating the calculated type of electron transition (l) and the summation in the denominator runs over possible i and j electron transitions with radiative Γ_{x_i} and nonradiative $\Gamma_{A_{ij}}$ emission rates taken from Scofield [48], while n_i, n_r, m_j are the numbers of remaining electrons on summed subshells for calculated type of electron transition, and N_i, N_r, M_j, are the numbers of electrons of fully occupied subshells in a neutral atom. This formula assumes that both the x-ray and Auger transition rates were scaled in proportion to the number of existing electrons in the particular subshells.

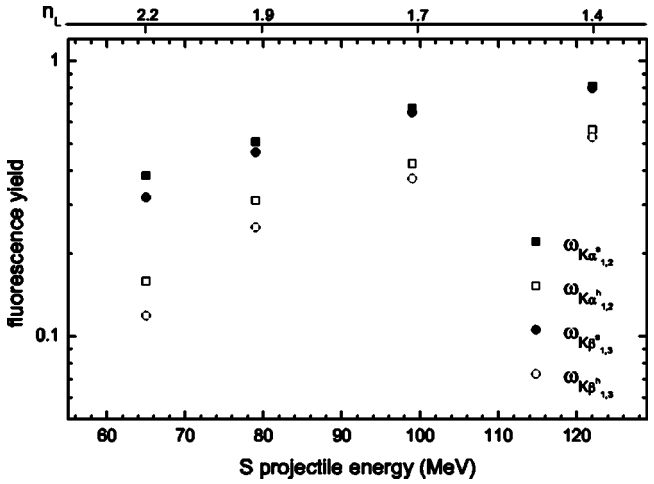

FIG. 3. The "effective fluorescence yields" for the highly ionized *S* projectiles emitting satellite $K\alpha_{1,2}^s$ (solid squares), $K\beta_{1,3}^s$ (solid circles), and hypersatellite $K\alpha_{1,2}^h$ (open squares), $K\beta_{1,3}^h$ (open circles) lines as a function of their energy. The top figure scale gives the average number of *L*-shell electrons remaining in the shell at the moment of x-ray emission.

Because of the lack of radiative and Auger emission rates for double *K*-shell vacancy configurations and highly excited states (with $4p$ and $5p$ electrons) the "effective fluorescence yields" were taken to be equal to the single *K* vacancy ones [37,49] and to the $3p$ electron configuration, respectively. Finally, the "effective fluorescence yield" for each of the measured lines (i.e., for projectiles in different electronic defect configuration) was estimated [30,43] as a sum of fluorescence yields of individual transitions creating this line in a multiple ionized ion normalized by the distribution of equilibrated projectile charge states [50]. The dependence of such estimated "effective fluorescence yields" for discussed lines on projectile energy is seen in Fig. 3. This procedure of fluorescence yields estimation was checked in our recent work [30] by applying these values for reliable reproduction of experimental *K* x-ray lines energy shifts which were predicted within the proposed model based on the multiconfiguration Dirac-Fock (MCDF) calculations [51]. The same estimation performed for multiply ionized Ar projectiles is in good agreement with the numerical calculations of Zou *et al.* [22] where the Hartree-Fock atomic model in the intermediate coupling scheme was used.

It is observed (Fig. 3) that the fluorescence yield increases by a factor of about 10 for the highest ion energy. The scale along the top of the Fig. 3 gives the average number of *L*-shell electrons existing in this shell at the moment of x-ray emission, evaluated according to our model based on MCDF

TABLE I. Experimental values of cross sections.

Energy (MeV)	Cross section (10^{-19} cm^2)											
	σ_{01}	σ_{12}	σ_{10}^{EC}	σ_{21}^{EC}	σ_{02}	σ_{20}	$\sigma_{\tau K\alpha^s}$	$\sigma_{\tau K\alpha^h}$	$\sigma_{\tau K\beta^s}$	$\sigma_{\tau K\beta^h}$	$\sigma_{\tau Ky^s}$	$\sigma_{\tau Ky^h}$
65	17.0	6.50	5.50	12.0	0.169	0.002	7.80	15.6	6.60	13.2		
79	19.5	7.36	6.50	14.0	0.185	0.002	6.00	12.0	5.10	9.90	4.70	9.40
99	22.0	9.78	5.20	10.4	0.190	0.002	4.75	9.50	4.07	8.14	3.75	7.50
122	24.0	10.5	4.40	8.80	0.192	0.002	3.36	6.82	3.20	6.62	3.00	6.20

calculations [30,52]. We would like to point out that the fluorescence yield depends on the ionization of the *L* and *M* shells and its value does not vary significantly with target thickness because the outer electrons equilibrate very rapidly [38]. Simultaneously, the multiple ionization of ions has been taken into account in the value of radiation probability per unit path length since $\lambda_l^{s,h}$ is a product of cross section for radiative and nonradiative filling process ($\sigma_{\tau l}$) and fluorescence yield ($\omega_l^{s,h}$).

The fit of the theoretical description (based on a three component model with zero, single and double *K*-shell vacancy fractions) to experimental $\sigma_{K\alpha_{1,2}^{s,h}}$, $\sigma_{K\beta_{1,3}^{s,h}}$ and $\sigma_{Ky^{s,h}}$ cross sections in function of penetration depth (see Fig. 2) shows that the dynamics of creation and disappearance of the projectiles with different number of *K*-shell electrons is determined by six charge-changing cross sections σ_{ij}. Physical processes responsible for the production of *K*-shell vacancies in projectile in collision with a target atom are described by σ_{01}, σ_{12} and σ_{02} production cross sections (in some works described by σ_v). Processes leading to the filling of *K*-shell vacancies, are presented by vacancy loss cross sections σ_{10}, σ_{21} and σ_{20} which represent the sum of the cross sections for electron capture to the adequate projectile *K*-shell vacancy (σ_{ij}^{EC}) and the cross sections for radiative and Auger decays ($\sigma_{\tau l}$).

The least-square fits [Eq. (5)] done independently for the experimental $\sigma K\alpha_{1,2}^s$, $\sigma K\alpha_{1,2}^h$, $\sigma K\beta_{1,3}^s$, $\sigma K\beta_{1,3}^h$, σKy^s, and σKy^h cross sections values (performed with the same values of σ_{01}, σ_{12}, σ_{02}, σ_{ij}^{EC}, and adequate values of $\sigma_{\tau l}$) give results shown by curves in Fig. 2. The agreement of predicted dependence of x-ray production cross sections on the carbon target thickness with the measured data is satisfactory. The numerical values of the cross sections which describe processes felt by the sulfur projectile inside the target, are listed in Table I.

The dependence of the experimental values of σ_{01}, σ_{12} and σ_{02} *K*-shell vacancy production cross sections of sulfur projectiles on their energy is given in Fig. 4. The results obtained have been compared with theoretical predictions for the direct *K*-shell ionization of sulfur ion by atom of carbon target, based upon PWBA model [53], which are also shown in Fig. 4. The theoretical estimations of σ_{ij} cross section have been performed for a "real" *K*-shell binding energy, expected for the most probable configurations of the multiply ionized sulfur projectiles [30,52], calculated using the MCDF method [51]. This binding energy correction caused a large reduction of the values of the calculated ionization cross sections. As it can be seen in Fig. 4 the discussed dependence of σ_{01} and σ_{12} *K*-vacancy production cross sections on the projectile energy [extracted from the fits of parameters of Eq. (5) to the experimental projectile x-rays production cross section] is in qualitative agreement with theoretical predictions for the direct *K*-shell ionization. However, the experimental σ_{01} and σ_{12} values are higher than theoretical ones by nearly an order of magnitude across the full range of projectile energy. The observed disagreement between experimental and theoretical values of the σ_{01} and σ_{12} cross sections indicates that some other mechanisms such as excitation play an important role in the *K*-shell vacancy production. On the basis of classical trajectory Monte Carlo (CTMC) calculations [54] it has been observed that for the examined ion-atom system the processes of electron excitation from *K* shell into higher atomic shells are much more probable than the direct *K*-shell ionization in the studied sulfur energy range. Thus, the CTMC predictions seem to explain the observed discrepancy. The conclusion that *K*-shell vacancy formation cross sections σ_{01}, σ_{12}, σ_{02} contain contributions from both ionization and excitation processes is in good agreement with the considerations and results of Gardner *et al.* [11] and Mizogawa *et al.* [23]. It can be noticed from Fig. 4 that the double vacancy production cross section σ_{02} plays an insignificant role in production of hypersatellite x rays. The double capture cross section σ_{20} should be small and was arbitrarily chosen to be much smaller than σ_{02}.

As mentioned above, the *K*-shell vacancy loss cross sections σ_{10} and σ_{21} are a result of two independent processes

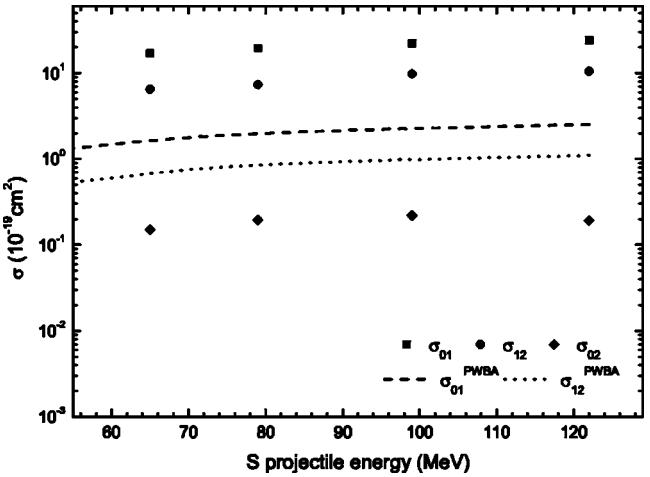

FIG. 4. Experimental σ_{01} (squares), σ_{12} (circles), and σ_{02} (diamonds) *K*-shell production cross sections together with the PWBA predictions (σ_{01}, dashed lines; σ_{12}, dotted lines) in function of the projectile energy.

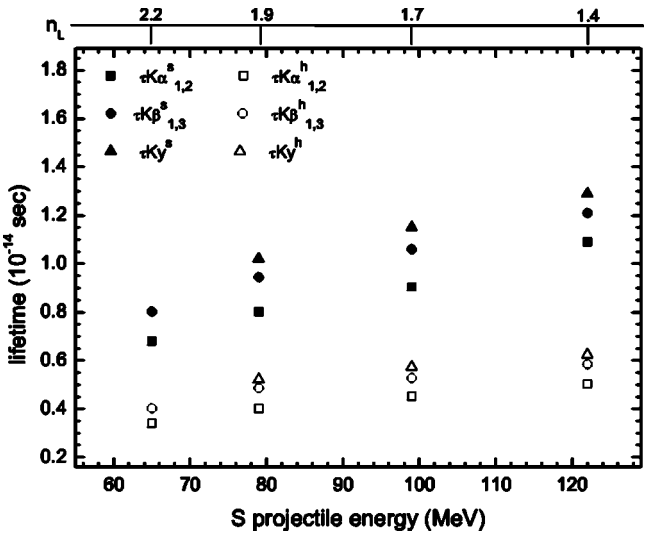

FIG. 5. Lifetimes of $K\alpha^s_{1,2}$ (solid squares), $K\beta^s_{1,3}$ (solid circles), and Ky^s (solid triangles) satellite, and $K\alpha^h_{1,2}$ (open squares), $K\beta^h_{1,3}$ (open circles), and Ky^h (open triangles) hypersatellite transitions in the sulfur ions traversing the carbon target. The axis at the top of figure describes mean number of *L*-shell electrons remaining in the ion at the moment of x-ray emission.

(see Table I), i.e., a filling of the *K*-shell vacancy *via* radiative or nonradiative electron transitions (adequate values of $\sigma_{\tau l}$ for each line) and an electron capture from target atoms into the *K*-shell vacancy of the projectile (σ^{EC}_{ij}). The filling cross section $\sigma_{\tau_l}=1/nv\tau_l$ is directly connected with the lifetime τ_l of the *K*-shell vacancy through the number *n* of target atoms per cm^3 and the projectile velocity v. Finally, the mean lifetimes τ_l for states which can emit satellite or hypersatellite lines extracted from fitted parameters of Eq. (5) to the projectile *K* x-ray production cross sections are presented in Fig. 5 in the function of the incident ion energy.

Experimentally determined lifetimes of sulfur ion states, from which satellite/hypersatellite x rays are emitted, increase with increasing projectile energy, which corresponds to the fact that the mean number of electrons in the ions decreases with increasing sulfur projectile energy. For the high ion energies presented in this work the number of sulfur ion electrons is small (<5) and therefore the transitions responsible for emission of $K\alpha^s_{1,2}$, $K\beta^s_{1,3}$, and Ky^s lines often come from different atomic states. The filling of the *K*-shell vacancy *via* radiative transitions plays an important role so that the lifetimes of the states emitting these transitions should be different [43]. It is interesting to notice that lifetimes of all hypersatellite states obtained for each discussed ion energy are about twice as short as for satellite ones. This seems reasonable since in the case of hypersatellite state the sulfur ion has two *K*-shell vacancies to be filled. Measured lifetimes of states emitting Ky^s and Ky^h lines are longer than these emitting $K\beta^{s,h}_{1,3}$ lines, respectively.

In Table II a comparison of our experimental lifetimes with the data from other works was shown. We have found a general agreement between these values. A good agreement is seen between our results and the ones obtained by Varghese *et al.* [55] for 49, 57, and 59 MeV sulfur energy and by Panke *et al.* [33,34] for 92 MeV sulfur projectiles. It should be noted that groups of Varghese and Panke used Doppler-tuned and Bragg spectrometers, respectively, to determine the lifetimes of the particular multiplet states, which are only a contribution to our $K\alpha^s$ line. The experimental lifetimes values extracted in the present study reflect decays of various states, contributions of which could not be resolved with the Si(Li) detector, and therefore the obtained τ_l values are the average lifetimes of all possible transitions which lead to the *K*-shell vacancy filling. The lifetime value of $(1s^12p^1)^1P$ state determined for the sulfur ions at 49, 57, 59 MeV is longer than that obtained by us for the sulfur projectiles at 65 MeV energy. Our latest considerations [30] show that this two-electron configuration is responsible only in 15% for $K\alpha^s_{1,2}$ line intensity, but the major contribution comes from the configurations $1s^12s^12p^1$(34%) and $1s^12s^22p^1$(30%) , for which the lifetimes of *K* vacancy are shorter than in the case of $1s^12p^1$ configuration. Consequently, the lifetime of 6.8×10^{-15} sec, determined by us as the mean lifetime for all possible transitions, is shorter than that for a single state $(1s^12p^1)^1P$, which can vanish only by radiative transitions. Analogically, in the case of 99 MeV ion energy the $1s^12p^1$ configuration contributes only 30% to $K\alpha^s_{1,2}$ line intensity, while the $1s^12s^12p^1$ configuration has also a large role (25%) in the production of this line, which results in a much lower value of mean lifetime of the *K* vacancy. Comparing our lifetime values (which describe the radiative and nonradiative processes) with the radiative data of Varghese *et al.* [55] and Panke *et al.* [33,34] we have to take into consideration the estimated values of the "effective fluorescence yields." We have found a small disagreement between the measured values of lifetime of the states emitting $K\alpha^s_{1,2}$ line in the case of 122 MeV energy with the results of Betz *et al.* [6] for the sulfur ions at 110 MeV energy. This discrepancy could be caused by using the two component model by Betz *et al.* [6], neglecting of the essential (for such high ion energy) double *K*-vacancy fraction of the ions (see Fig. 7).

Calculations for the electron capture cross section σ^{EC}_{ij} have been performed using the Oppenheimer-Brinkmann-Kramers (OBK) formulation of electron exchange by Nikolaev [56] given by Lapicki and McDaniel [57]. These cal-

TABLE II. The experimental mean lifetimes of the states, emitting the $K\alpha^s_{1,2}$ or $K\beta^s_{1,3}$ transitions and lifetimes of the states from other works.

Energy (MeV)		Lifetimes (sec)	References
65	$K\alpha^s_{1,2}$	6.8×10^{-15}	Present
49, 57, 59	$(1s^12p^1)^1P$	1.2×10^{-14}	Varghese [55]
99	$K\alpha^s_{1,2}$	9.05×10^{-15}	Present
	$(1s^12p^1)^1P$	1.7×10^{-14}	
92	$(1s^12p^2)^2P$	9.0×10^{-15}	Panke [33,34]
	$(1s^12p^2)^2D$	9.0×10^{-15}	
122	$K\alpha^s_{1,2}$	1.09×10^{-14}	Present
110	$K\alpha^s_{1,2}$	1.4×10^{-14}	Betz [6]
122	$K\beta^s_{1,3}$	1.21×10^{-14}	Present
110	$K\beta^s_{1,3}$	3.3×10^{-14}	Betz [6]

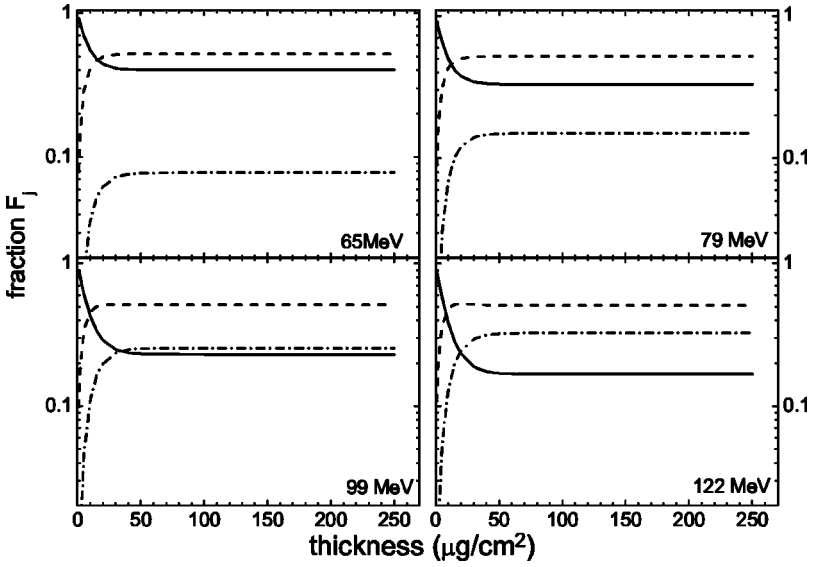

FIG. 7. The dependence of magnitude of fraction with zero (solid lines), one (dashed lines) and two (dash dotted lines) *K*-shell vacancies on the depth of target penetration for the case of entering sulfur projectiles with a fully occupied *K* shell.

culations give the total electron capture cross section from all shells of the target atoms to the projectile *K*-shell with a single (σ_{10}^{EC}) or with two vacancies (σ_{21}^{EC}), respectively. Contrary to the work of Gardner *et al.* [11] or Cocke *et al.* [38] no scaling factor has been introduced to the calculated values of both cross sections. In our calculations we have used again the "real" *K*-shell binding energy. The comparison of calculated and experimental σ_{ij}^{EC} cross sections is shown in Fig. 6. The obtained experimental values of σ_{10}^{EC} and σ_{21}^{EC} cross sections are higher than the theoretical predictions in the full range of the sulfur projectile energy. This disagreement seems to be connected with the inadequacy of the theoretical description of the very complicated situation of an ion passing through a carbon target. In particular, the theoretical model does not take into account the capture of free electrons from a target.

The experimental values of all σ_{ij} cross sections obtained from the least-square fit have been used to determine the dynamics of formation of the *K*-shell vacancy fractions of sulfur projectiles passing through a carbon foil. The dependence of the magnitude of fractions with zero, one and two *K*-shell holes on the depth of target penetration is presented in Fig. 7 for the case of entering sulfur projectiles with a fully occupied *K* shell. As can be seen, for all projectile energies with increasing depth of target penetration the fraction with zero *K*-shell vacancies (F_0) disappears and the fractions with single (F_1) and double (F_2) *K*-shell vacancies increase until they reach the equilibrium state. This state is achieved by the sulfur ions after coming through the characteristic target depth for each ion energy: for the lower energies (65–79 MeV) it is equal $\sim 50\ \mu g\ cm^{-2}$ and for the higher ones it is over $\sim 70\ \mu g\ cm^{-2}$. It is very interesting that the magnitude of F_0 and F_2 fractions in the equilibrium condition depends strongly on beam energy. As can be seen, the F_0 fraction strongly and systematically decreases from $\sim$40% for 65 MeV up to $\sim$17% for 122 MeV. Simultaneously, the F_2 fraction becomes substantial for the projectile with the measured energies and increases from $\sim$8% for 65 MeV to $\sim$30% for 122 MeV. However, the contribution of F_1 fraction in the equilibrium condition is close to $\sim$50% for the beam energy in 65–122 MeV region.

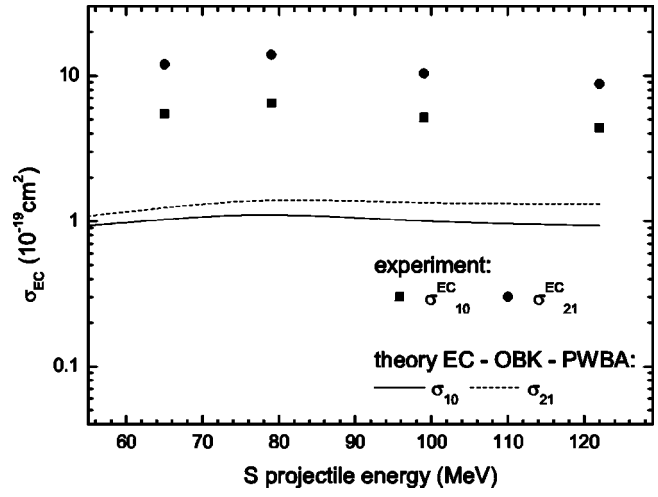

FIG. 6. The comparison of experimental and theoretical electron capture cross sections σ_{ij}^{EC}.

V. SUMMARY AND CONCLUSIONS

The dependence of the satellite and hypersatellite sulfur *K* x-ray production cross sections on the target thickness has been examined, separately for each line recorded in spectra of characteristic x rays of the projectiles at energy range of 65–122 MeV. The three component model, which expresses the probability of an ion charge-changing collisions by the cross sections σ_{ij} was used. For each sulfur projectile energy the values of the *K*-shell vacancy production cross sections and the *K*-shell vacancy loss cross sections (independently for the electron capture and for the radiative and Auger decays) have been fitted. The obtained experimental values of all σ_{ij} cross sections have been used later to determine the dynamics of formation of the *K*-vacancy fractions of the sulfur projectiles passing through a carbon foil.

On the basis of the presented study some general conclusions can be drawn. The obtained from the least-square fit

"experimental" values of the σ_{01} and σ_{12} *K*-vacancy production cross sections, much higher than the theoretical (PWBA) predictions, suggest that apart from the direct *K*-shell ionization process some other mechanisms such as excitation play an important role in the *K*-shell vacancy production. This suggestion has been confirmed by the results of recent calculations in the framework of the CTMC model, where it has been observed that for the examined ion-atom system the processes of electron excitation from *K* shell into higher atomic shells are much more probable than the direct *K*-shell ionization in the studied sulfur energy range. It is worth noticing that there is an independent experimental confirmation of the significant role of excitation processes. This is the appearance of the Ky^h peak in the measured spectra of sulfur ions passing through carbon foils, which proves that very high 4*p* and 5*p* subshells (unoccupied in the ground state of neutral sulfur atom) are occupied during the excitation processes. Moreover, it was found that two *K*-shell vacancies are mainly produced in a two step process ($\sigma_{01} \rightarrow \sigma_{12}$) and the σ_{02} cross section plays an insignificant role in the production of hypersatellite x rays. An enhancement of the experimental σ_{10}^{EC} and σ_{21}^{EC} cross section values over the theoretical predictions (PWBA-OBK) indicates a special role of the solid state effect and the capture of free electrons from the target. We must here realize that the three component model used in our study, although very sophisticated, cannot take into account the full complexity of the occurring processes.

The estimated mean lifetimes τ_l (which are directly connected with the *K*-shell vacancy filling *via* radiative or nonradiative electron transitions cross sections) for states, which can emit satellite or hypersatellite lines, increase with increasing projectile energy. This behavior is a result of the fact that the mean number of electrons in the ions decreases with increasing sulfur energy. The lifetimes of the states responsible for emission of the $K\alpha_{1,2}^{s}$ line are shorter than that for the $K\beta_{1,3}^{s}$ line, since these lines come mostly from different atomic states. Furthermore, it was obtained that the lifetimes of hypersatellite states are about twice as short as the satellite lifetimes because the hypersatellite state of the sulfur ion has two *K*-shell vacancies to be filled. The last conclusion is that for all projectile energies with an increasing depth of the foil penetration the fraction with zero *K*-shell vacancies (F_0) disappears and the fractions with single (F_1) and double (F_2) *K*-shell vacancies increase until they reach the equilibrium state. The magnitude of F_0 and F_2 fractions in the equilibrium condition strongly depends on the ion energy, i.e., the F_0 fraction systematically decreases from $\sim$40% for 65 MeV to $\sim$17% for 122 MeV and F_2 fraction systematically increases from $\sim$8% for 65 MeV to $\sim$30% for 122 MeV. However, the contribution of F_1 fraction in the equilibrium condition is close to $\sim$50% for all studied beam energies.

ACKNOWLEDGMENTS

This work was supported by the Federal Ministry for Research and Technology, Germany, under Contracts No. N-88-94 and No. POL-017-98, and by the Polish State Committee for Scientific Research under Grants No. 2P03B 094 24, No. 2P03B 038 24, and No. 1P03B 046 26. We wish to express our appreciation to the staff of the U-200P cyclotron at the Heavy Ion Laboratory of the Warsaw University for their kind collaboration during the measurements.

[1] P. H. Mokler and F. Folkmann, in *Structure and Collisions of Ions and Atoms*, edited by I. A. Sellin (Springer-Verlag, Berlin, 1978), p. 201.
[2] J. McWherter, J. Bolger, C. F. Moore, and P. Richard, Z. Phys. **263**, 283 (1973).
[3] R. L. Kaufman, J. H. McGuire, P. Richard, and C. F. More, Phys. Rev. A **8**, 1233 (1973).
[4] R. L. Watson, F. E. Jenson, and T. Chiao, Phys. Rev. A **10**, 1230 (1974).
[5] P. Rymuza, Z. Sujkowski, M. Carlen, J-Cl. Dousse, M. Gasser, J. Kern, B. Penry, and Ch. Rheme, Z. Phys. D: At., Mol. Clusters **14**, 37 (1989).
[6] H. D. Betz, F. Bell, H. Panke, G. Kalkoffen, M. Welz, and D. Evers, Phys. Rev. Lett. **33**, 807 (1974).
[7] F. Hopkins, Phys. Rev. Lett. **35**, 270 (1975).
[8] K. O. Groeneveld, B. Kolb, J. Schader, and K. D. Sevier, Z. Phys. A **277** 13 (1976).
[9] T. J. Gray, P. Richard, K. A. Jamison, and J. M. Hall, Phys. Rev. A **14**, 1333 (1976).
[10] F. Hopkins, J. Sokolov, and A. Little, Phys. Rev. A **15**, 588 (1977).
[11] R. K. Gardner, T. J. Gray, P. Richard, C. Schmiedekamp, K. A. Jamison, and J. M. Hall, Phys. Rev. A **15**, 2202 (1977).
[12] J. A. Tanis, W. W. Jacobs, and S. M. Shafroth, Phys. Rev. A **22**, 483 (1980).
[13] B. B. Dhal, H. C. Padhi, K. G. Prasad, P. N. Tandon, and M. Polasik, J. Phys. B **31**, 1225 (1998).
[14] P. H. Mokler, Phys. Rev. Lett. **26**, 811 (1971).
[15] C. W. Woods, F. Hopkins, R. L. Kauffman, D. O. Elliott, K. A. Jamison, and P. Richard, Phys. Rev. Lett. **31**, 1 (1973).
[16] R. L. Watson, J. R. White, and F. E. Jenson, Phys. Lett. **67A**, 269 (1978).
[17] R. L. Watson, J. R. White, A. Langenberg, R. A. Kenefick, and C. C. Bahr, Phys. Rev. A **22**, 582 (1980).
[18] Y. Awaya, T. Kambara, M. Kase, H. Shibata, H. Kumagai, K. Fujima, J. Urakawa, T. Matsuo, and J. Takahashi, Nucl. Instrum. Methods Phys. Res. B **10/11**, 53 (1985).
[19] K. Shima, K. Umetani, and T. Mikumo, Nucl. Instrum. Methods Phys. Res. **194**, 353 (1982).
[20] H. J. Hay, L. F. Pender, and P. B. Treacy, Aust. J. Phys. **34**, 155 (1981).
[21] H. J. Hay, L. F. Pender, and P. B. Treacy, Nucl. Instrum. Methods Phys. Res. **194**, 349 (1982).
[22] Y. Zou, Y. Awaya, C. P. Bhalla, T. Kambara, Y. Kanai, M. Oura, Y. Nakai, K. Ando, A. Hitachi, and S. Kravis, Phys. Rev. A **51**, 3790 (1995).

[23] T. Mizogawa, Y. Awaya, T. Kambara, Y. Kanai, M. Kase, H. Kumagai, P. H. Mokler, and K. Shima, Phys. Rev. A **42**, 1275 (1990).
[24] H. F. Beyer, H. J. Kluge, and V. P. Shevelko, *X-Ray Radiation of Highly Charged Ions, Springer Series on Atoms and Plasmas* (Springer-Verlag, Berlin Heidelberg, New York, 1997).
[25] M. Pajek, D. Banaś, J. Braziewicz, U. Majewska, J. Semaniak, T. Czyżewski, M. Jaskóła, W. Kretshmer, T. Mukoyama, D. Trautmann, and G. Lapicki, in *Application of Accelerators in Research and Industry*, edited by J. L. Duggan and I. L. Morgan, AIP Conf. Proc. No. 475 (AIP, Woodbury, NY, 1999), p. 32.
[26] D. Banaś, M. Pajek, J. Semaniak, J. Braziewicz, A. Kubala-Kukuś, U. Majewska, T. Czyżewski, M. Jaskóła, W. Kretschmer, T. Mukoyama, and D. Trautmann, Nucl. Instrum. Methods Phys. Res. B **195**, 233 (2002).
[27] D. Banaś, J. Braziewicz, U. Majewska, M. Pajek, J. Semaniak, T. Czyżewski, M. Jaskóła, W. Kretschmer, and T. Mukoyama, Nucl. Instrum. Methods Phys. Res. B **154**, 247 (1999).
[28] D. Banaś, J. Braziewicz, A. Kubala-Kukuś, U. Majewska, M. Pajek, J. Semaniak, T. Czyżewski, M. Jaskóła, W. Kretschmer, and T. Mukoyama, Nucl. Instrum. Methods Phys. Res. B **164-165**, 344 (2000).
[29] D. Banaś, J. Braziewicz, U. Majewska, M. Pajek, J. Semaniak, T. Czyżewski, M. Jaskóła, W. Kretschmer, T. Mukoyama, and D. Trautmann, J. Phys. B **33**, L793 (2000).
[30] U. Majewska, K. Słabkowska, M. Polasik, J. Braziewicz, D. Banaś, T. Czyżewski, I. Fijał, M. Jaskóła, A. Korman, and S. Chojnacki, J. Phys. B **35**, 1941 (2002).
[31] R. L. Watson, J. M. Blackadar, and V. Horvat, Phys. Rev. A **60**, 2959 (1999).
[32] R. L. Watson, V. Horvat, J. M. Blackadar, and K. E. Zaharakis, Phys. Rev. A **62**, 052709 (2000).
[33] H. Panke, F. Bell, H. -D. Betz, H. Stehling, E. Spindler, and R. Laubert, Phys. Lett. **53A**, 457 (1975).
[34] H. Panke, F. Bell, H. D. Betz, and H. Stehling, Nucl. Instrum. Methods **132**, 25 (1976).
[35] J. A. Tanis and S. M. Shafroth, Phys. Rev. Lett. **40**, 1174 (1978).
[36] U. Scharfer, C. Henrichs, J. D. Fox, P. Von Brentano, L. Degener, J. C. Sens, and A. Pape, Nucl. Instrum. Methods **146**, 573 (1977).
[37] T. J. Gray, C. L. Cocke, and R. K. Gardner, Phys. Rev. A **16**, 1907 (1977).
[38] C. L. Cocke, S. L. Varghese, and B. Curnutte, Phys. Rev. A **15**, 874 (1977).
[39] S. K. Allison, Rev. Mod. Phys. **30**, 1137 (1958).
[40] J. P. Biersack and L. G. Maggmark, Nucl. Instrum. Methods **174**, 257 (1980).
[41] J. Ziegler, http://www.srim.org
[42] M. Pajek, A. P. Kobzev, R. Sandrik, R. A. Ilkhamov, and S. A. Khusmorodov, Nucl. Instrum. Methods Phys. Res. B **42**, 346 (1989).
[43] U. Majewska, J. Braziewicz, M. Polasik, K. Słabkowska, I. Fijał, M. Jaskóła, A. Korman, S. Chojnacki, and W. Kretschmer, Nucl. Instrum. Methods Phys. Res. B **205**, 799 (2003).
[44] J. A. Bearden, Rev. Mod. Phys. **39**, 78 (1967).
[45] M. O. Krause, J. Phys. Chem. Ref. Data **8**, 307 (1979).
[46] J. H. Scofield, Phys. Rev. A **9**, 1041 (1974).
[47] F. P. Larkins, J. Phys. B **4**, L29 (1971).
[48] J. H. Scofield, At. Data Nucl. Data Tables **14**, 121 (1974).
[49] J. A. Tanis, S. M. Shafroth, J. E. Willis, and J. R. Mowat, Phys. Rev. Lett. **45**, 1547 (1980).
[50] K. Shima, N. Kuno, M. Yamanouchi, and H. Tawara, At. Data Nucl. Data Tables **51**, 173 (1992).
[51] M. Polasik, Phys. Rev. A **58**, 1840 (1998).
[52] U. Majewska, J. Braziewicz, D. Banaś, M. Jaskóła, T. Czyżewski, W. Kretschmer, K. Słabkowska, F. Pawłowski, and M. Polasik, Acta Phys. Pol. B **31**, 511 (2000).
[53] W. Brandt and G. Lapicki, Phys. Rev. A **20**, 465 (1979); **23**, 1717 (1981).
[54] K. Słabkowska, M. Polasik, and M. Janowicz, Phys. Rev. A **67**, 012713 (2003).
[55] S. L. Varghese, C. L. Cocke, B. Curnutte, and G. Seaman, J. Phys. B **9**, L387 (1976).
[56] V. S. Nikolaev, Zh. Eksp. Teor. Fiz. **51**, 1263 (1966) [Sov. Phys. JETP **24**, 847 (1967)].
[57] G. Lapicki and F. D. McDaniel, Phys. Rev. A **22**, 1896 (1980).